International Journal of Latest Engineering Research and Applications (IJLERA) ISSN: 2455-7137

Volume – 10, Issue – 03, March 2025, PP – 19-31

Seismic and Induction Transducers, Misaligment

P. Fraga,[1] B. F. De Cal, B.[2]

[1]*PhD Mechanical Engineer, A Coruña University, Spain*
Higher Polytechnic School, Department of Industrial and Naval Engineering
C./Mendizabal s/n 15403 Ferrol (A Coruña), Spain
[2]*PhD Mechanical Engineer, MSc Sustainable Energy Systems of Queen Mary University of London*

Abstract: This paper presents a successful application, among many others, of industrial mechatronics on the quality and proper functioning of rotating machines. The misalignment is the most common latent anomaly in a rotating system after imbalance, so this phenomenon is chosen.

The information that a seismic transducer can give of the vibration of a rotor is compared with that provided by the installation of two induction transducers or proximity, located in transverse planes at 90º, which not only reproduce a high vibration alarm, but also provide important information about the causes. This study has been carried out in a laboratory rotor, causing the phenomenon of misalignment.

Latent misalignment is therefore very dangerous, because the cyclic charges can produce microscopic surface discontinuities that act as tension concentrated, and therefore, as nucleation sites of cracks. Subsequently, a radial load will be introduced which and increased in progressive values to simulate the load that the misalignment would produce, and thus the vibration propagation will be observed, comparing seismic and proximity transducer data.

Keywords: Rotor dynamics, vibration, misalignment, seismic and proximity transducers.

1. Introduction

Misalignment may not manifest itself at first and remain latent, so that with the normal wear of bearings, mechanical seals or other supports, it aggravates and causes major damage to these machines. Produces significant strengths in shafts, bearings and couplings that varies at the frequency of rotor speed.

A further consequence of the effects of shaft misalignment is the generation of external radial loads in a specific direction, which forces the shaft to one side. The movement of a shaft with this phenomenon is represented by [1]:

$$Mx" + D_x(1-\lambda_x)x' + K_x x + \ + K_{rx}(\Omega)y = mr\Omega^2\, cos[(\Omega t+\delta)\,] + P\, cos\gamma \quad (1)$$

$$My" + D_y(1-\lambda_y)y' + K_y y + K_{ry}(\Omega)x + y(K_n y + \cdots \ldots = \ mr\Omega^2\, sin(\Omega t+\delta) + P\, sin\gamma \quad (2)$$

where x(t) and y(t) are the deflections of the shaft in the horizontal and vertical direction; t is time; M, D and K are respectively the mass, damping and rigidity of the rotor considered; m, r, and δ are the mass of disequilibrium that always exists, the radius and the angular position of it; P is the radial load of the assumed misalignment, γ is the angle of incidence of the P radial load from the misalignment, and K_n is a nonlinear stiffness coefficient, that appears in the misalignment plane, as a consequence of this displacement of the rotor in that plane and λ, Ω are fluid circumferential average velocity ratio and rotor rotational speed respectively.

The equation (1) and (2) contains, therefore, the stiffness-related non-linear term which represents only an example of nonlinearities that may be active in the system, as fluid film radial stiffness and damping at high eccentricities have different functional form of nonlinearities, that may be referred to as the first term of the Taylor development for any nonlinear function (the dots indicate possible existence of the other nonlinear terms).

It is believed that only that the only nonlinearity in the system has the quadratic form. Due for to nonlinearity, the rotor response vibration contains not only synchronous component but also higher harmonics, 2X, 3X, etc., so these equations (1)and (2) can be expressed as the following, for a simple symmetrical rotor model, that we now suppose applied, this misalignment and load radial P, in the vertical plane, exclusively:[2]

$$Mx" + D_x x' + K_X x \ = mr\Omega^2\, cos[(\Omega t+\delta)\,] \quad (3)$$

$$My" + D_y y' + K_y y + K_n y^2 = \ mr\Omega^2\, sin(\Omega t+\delta) + P \quad (4)$$

And solutions of equations (3) and (4) is assumed as:[2]

$$x(t) = \ A_x \cos(\Omega\, t + \alpha_x) \quad (5)$$

$$y(t) = \ A_0 + A_1 \,\mathrm{sen}(\Omega\, t + \alpha_1) + A_2 \,\mathrm{sen}(2\Omega\, t + \alpha_2), \quad (6)$$

In which the response 2X is already observed, in the assumed vertical plane of the misalignment, P is the force, A_2 is the amplitude, 2Ω is the frequency, α_2 is the phase angle and A_0 is the static displacement to the rotor stopped because of the deflection of the shaft in that plane caused by the lateral force of the misalignment P, that does not occur in another plane. That is, we will have a significant 1X synchronic response in both planes and a 2X response only in the misaligned plane, which means that they are presented an asymmetric response in the two planes and an important 1X response because the mass modification caused by a shaft asymmetrical from its center is important.

A misaligned shaft would have the shape of the Figure 1 and the forces that occur are:

- F_1 and F_2 = load on bearing to oppose bending forces.
- P = vertical force resulting from bending forces.
- M_A and M_B = bending torque resulting from bending forces.
- N = axial thrust on the shaft.

All these forces are induced from bending shaft, in addition to some axial vibration as shown by the appearance of the alternative force N according to the decomposition of forces of the Figure 1 and Figure 2Figure 2, although it is not analyzed in this study.

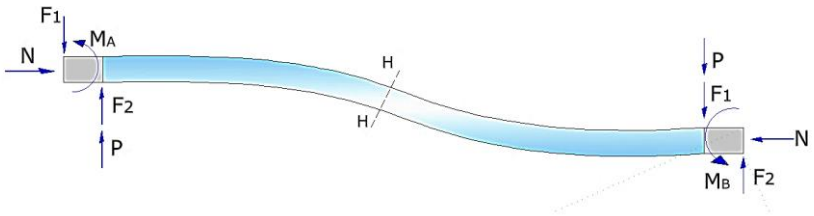

Figure 1: Misalignment shaft.

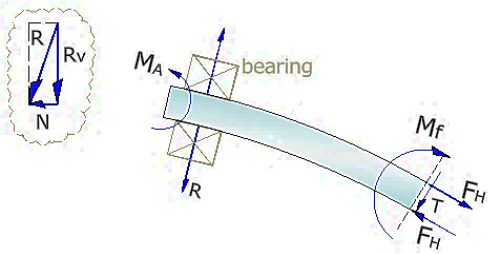

Figure 2: Strength decomposition on misaligned shaft.

External, non-rotating preloads, such as a misalignment, can also be produced by gravity on a horizontal machine, a pressure charge of gas or steam by a nozzle, air in a compressor, hydraulics in a pump or even the action of engaging gears under conditions of external misalignment, distorts the shape of an almost circular orbit to "elliptical", "banana" or "eight" shapes according to Figure 3.

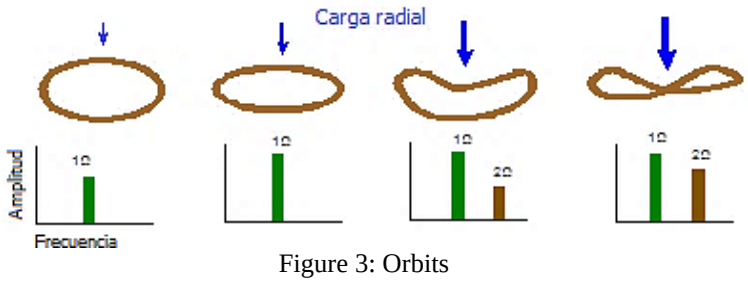

Figure 3: Orbits

The second resonance (2X), has the following amplitude value A_2, equation (7) and its frequency of this resonance given by the equation (8),[2]:

$$A_{2(res)} = \frac{K_n\, A_1^2}{2D\sqrt{\sqrt{1+4\frac{P\,K_n}{K^2}}}}\sqrt{\frac{M}{K}} \tag{7}$$

$$\Omega_{res} = \left(\frac{\Omega_{res}}{2}\right) \equiv \frac{1}{2}\sqrt{\frac{K}{M}}\sqrt{\sqrt{1+4PK_n/K^2}} \tag{8}$$

It is observed that the 2X response presents a resonance at a frequency equal to half the value of the critical velocity. The expression under the two radicals represents the non-linearity with respect to the natural frequency of the system √(K/M), as well as for the first resonance1X, we will have: [2]

$$A_{1(res)} = \frac{m\,r}{D}\sqrt{\frac{K}{M}}\sqrt{\sqrt{1+4\frac{P\,K_n}{K^2}}} \tag{9}$$

$$\Omega = \Omega_{res} \equiv \sqrt{\frac{K}{M}}\sqrt{\sqrt{1+4PK_n/K^2}} \tag{10}$$

Consequently, according to the expressions of the analyzed mathematical model of misalignment, which is a single rotor model (Figure 4 and Figure 5), but which provide its values with respect to other parameters and, above all, with respect to the rotation speed of the machine. The following can be highlighted:

- The amplitude A_0 of the static displacement depends fundamentally on the radial load P, which occurs only in the plane of misalignment.
- The amplitude of the 1X response (A_1), which corresponds to the unique situation of a stabilized rotor with the controlled residual unbalance that will always exist, is directly proportional to the mass "m" of unbalance and its radial position "r", and inversely proportional to the damping of system D, as seen in equation (9). This response will present a single amplitude of resonance and phase change, at the critical speed of the system Ω_{res}.
- The amplitude of the 2X (A_2) response is proportional to the square of the amplitude of the 1X (A_1^2) response, equation (7). This means that, in addition to a resonance at half the critical velocity, $\Omega_{res}/2$, as seen in equation(8), this 2X response will present another amplitude maximum simultaneous to the resonance that is present in the 1X response, i.e., to the Ω_{res}.
- This 2X response will therefore present two maximum resonance amplitude and two-phase changes: one at half the critical velocity, $\Omega_{res}/2$, and one at the critical velocity, Ω_{res}.

The causes more commons of misalignment are:[3]

- Incorrect cold alignment.
- Unexpected thermal growth.
- Support movement.
- Piping strain.
- Bearing wear.
- Coupling alignment.

When a rotor system with hydrodynamic bearings changes speed or load, the stiffness and damping characteristics of the bearings are also modified. As a result, changes in the average radial position of the shaft will also be observed, by the aforementioned installation of two induction transducers at 90º in their cross-section.

Primary and secondary machinery malfunctions such as misalignment, fluid-induced instability, and rubs, to name a few, can produce significant changes in the rotor's radial position within the bearings and/or seals. These changes in radial shaft position can be directly observed through the average shaft centerline data plot.

Correlation of shaft average centerline data with other vibration and process data provides a much more complete understanding of the total response of the rotor system. Thus, it is important to recognize that changes

in shaft radial position are just as important an indicator of machinery health as changes in the dynamic motion (vibration) of the rotor and must not be overlooked during the analysis.
Radial preloads include the following:

- Gravity is the most common preload caused on a horizontal rotor.
- Fluid forces can act as preloads by single volute pump, turbine partial steam admission, turbine gas admission, etc.
- Bearing wear, curvature of pad in a tilting pad bearing, etc.
- External misalignment by cold mounting.
- Pipes strain.

2. Experiment and Case Study

A test is carried out on a study rotor, such as the one in Figure 4 and Figure 5Figure 1, in which a grinding of 50 to 100 μm has been carried out, on the support 3 to simulate a misalignment in the vertical plane. 90º induction transducers are also installed in the (x) and (y) axes, as well as seismic transducers or accelerometers on the pedestal, in order to obtain a comparison of the measurements of both types of transducers, although really, the decision to use one or the other transductor depends a lot on the relative stiffness of the bearings [4].

The dimensions are 165 x 340 x 789 mm, shaft diameter of 9.5 mm and maximum speed of 10000 rpm. It also has a coupling device to the shaft, that constitute a mechanical seal or bearing in a pressurized fluid environment contained in a transparent polycarbonate shell, and its accessories: two induction transducers.

Figure 4: Test Rotor Set

The dynamic system of rotation that is analysed can be assimilated to the possible failures in a rotor of tests like the Figure 4[5], and that it is chosen to know from it its mechanical characteristics in order to perform and obtain real numerical calculations, on that model, which will always be more explicit. It consists of a mechanical foundation that includes a dc-electric drive motor, a shaft-rotor with test discs, bearings, six magnetic induction transducers, three probe assemblies and a safety cover of polycarbonate.
Instrumentation and equipment are also available, such as:

- Spectrum analyser with 208-P data acquisition unit, computer and analyser software with graphic presentation of vibrations for Windows. The graphs that this analyser displays on the computer are: shaft orbits, diagrams on the basis of time, trend diagrams, XY graphs, vector tabulation, Nyquist polar diagrams, Bode diagrams, shaft centre position and cascade spectra.
- Digital vector filter for selection of responses to the 1X disturbance.
- Two oscilloscopes for analysis of the position of the shaft centre.
- Speed control instrumentation, oil pump, cooling system, two thermometers.
- Laser aligner "Easy Laser Shims". Brookfield digital Viscometer. Manometer from 0 to 700 kPa,
- and another phase reference, plus a load spring frame to simulate shaft eccentricities.

The model of rotor to perform this test, is indicated in the plot of Figure 5, where: 1.- 75W cc drive motor, 2.- flexible coupling, 3a and 3b.- antifriction/bronze bearings, 4.- 1.63 kg disc-rotor, 5.- shaft centring support with four springs, 6.- aluminium disc for controlled imbalances, 7.- mechanical seal of 50 mm in length with radial clearance of 220μm and a circuit pressure of 10342 Pa, 8.- pressurized oil circuit in the gap of the seal, 9.- horizontal and vertical induction transducers, 10.- phase reference transducer, 11.- seismic transducer, 12.- horizontal and vertical induction transducers, 13.- seismic transducer.

The characteristics of this test rotor, before originating the misalignment in the shaft, that were calculated as indicated [6], are:

- Natural rotor frequency, without crack, 2260 rpm.
- Modal stiffness coefficient, K = 10,65 KN/m.

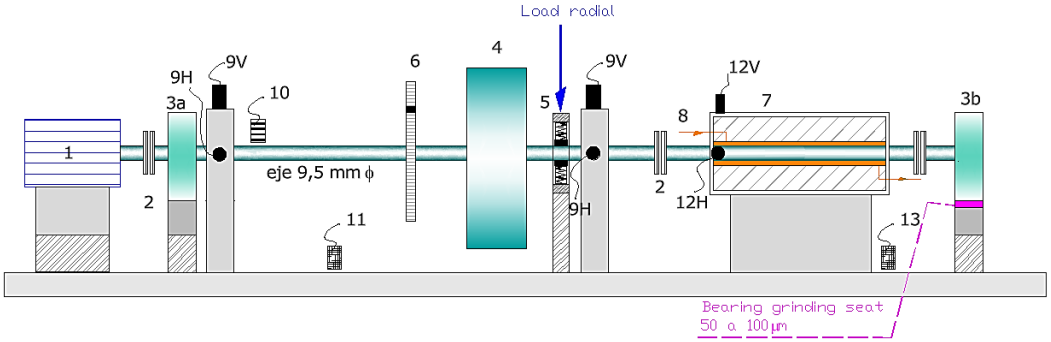

1: electric motor 0,1 HP; 2: Flexible coupling; 3a, 3b: bearing; 4: rotor mass 1,60 kg; 5: spring frame; 6: unbalanced disc; 7: oil lubricate seal; 8: oil circuit; 9: proximity transducer, horiz.&vert.; 10: phase reference, 11: sismic transducer, 12: proximity transducer, horiz.&vert., 13: sismic transducer.

Figure 5: Rotor-kit.

Thanks to having two induction or proximity transducers in the x-y axes (

Figure 6), we can have other graphic presentations that provide us with the possible cause of the high vibration, such as the position of the center of the shaft and the orbit it develops, according to the Figure 7.

An important sign of misalignment is the position in contraposed quadrants of the center of the shaft, as can be observed in the Figure 7.The orbit of the center of the shaft goes into abnormal situations, due to the radial overload that the misalignment imprints on it, the orbit changes from an “elliptical” shape to a "banana" shape, which indicates that vibration components of higher frequencies than the synchronous one appear. In that Figure 7, the preloads on the shaft force it, in one bearing, to position its orbit in the upper quadrant, and in the other bearing, to do so in the lower quadrant.

Many vibration characteristics associated with highs vibration levels can only observed by using induction transducers, as are:

- Shaft average centreline position.
- Shaft orbital motion.
- Direction of shaft orbital precession.

In addition to this 50 µm grinding in bearing 3bV, with the spring box "5" of the Figure 5 the shaft with a radial preload P, external in this case, is forced to be off-centre from the bearing hole before the rectification, to the new clearance with the 50 µm made.

The polar orbits of Figure 8 are then obtained, for bearing 3a, without a seat, and for bearing 3b, with the seat marked from 50 µm, from the XY induction transducers according

Figure 6[7], and its indicates that a large load occurred at bearing 3b[8]. As a consequence of the asymmetry between the dynamic stiffness in the X and Y direction of the bearings and the load introduced in the vertical direction Y, the orbit of the shaft precessions in an elliptical shape with an axis greater than 48º in the horizontal plane, in addition to the fact that this orbit of the shaft becomes much more elliptical in that bearing 3b, in which the vertical desalination load is applied, while in bearing 3a, without seat, the orbit is much more circular (Figure 8).

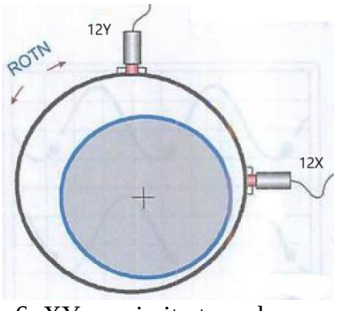

Figure 6: XY proximity transducers at 90º.

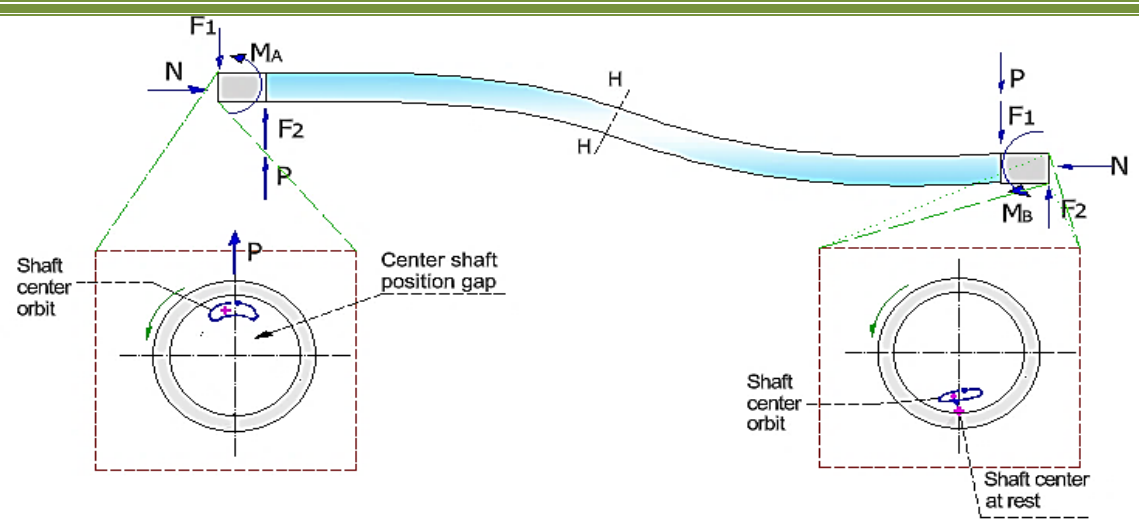

Figure 7: Excessive radial preload. Orbits and centreline position

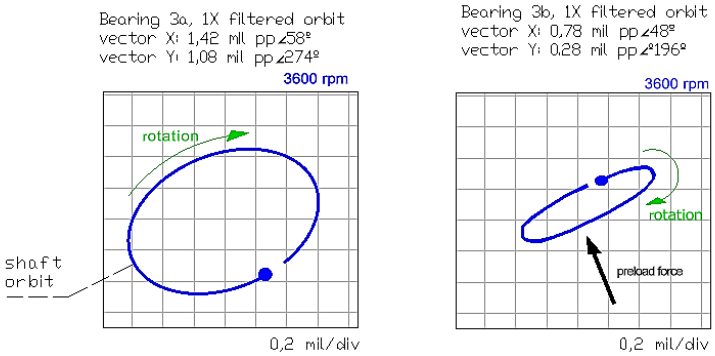

Figure 8: 1X filtered orbit plot

Preloads will tend to change the average position of the shaft within the clearance. The initial response is a change in the 1X response and when the preload has increased to distort the orbit, then 1X, 2X, etc and possibly reverse precession will appear.

Something similar to bearing 3b occurs in the mechanical seal due to forced misalignment, according to the 12X and 12Y transducers, where the inside of that seal, lubricated by fluid under oil pressure looks like the Figure 9 and Figure 10[9], which shows a simplified model used to derive a method for experimentally estimating the journal bearing stiffnesses, using exclusively the monitored shaft relative and the bearing absolute vibrations. In this Figure 9, (x_s, y_s), (x_b, y_b), and (x_f, y_f) are, respectively, the coordinates of the shaft, the seal, and the foundation; f_x and f_y are the components of the rotating force in X-direction and Y-direction. This model considers that the foundation vibrations are negligible.

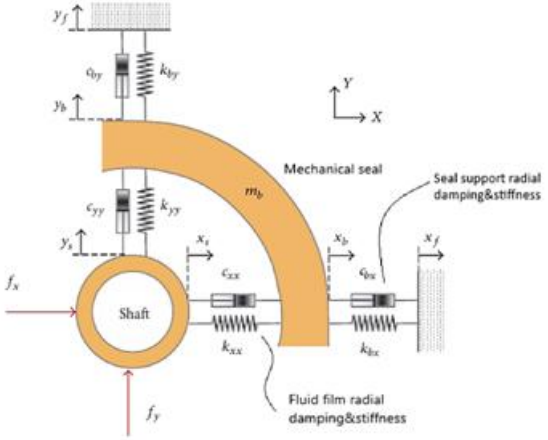

Figure 9: Journal mechanical seal stiffness and damping

Direct oil film stiffnesses in *X*-direction and *Y*-direction are, respectively, k_{xx} and k_{yy}, while direct damping coefficients are c_{xx} and c_{yy}.Cross-coupled stiffnesses (k_{xy}, k_{yx}) and damping (c_{xy}, c_{yx}) coefficients are preliminarily considered. Stiffness and damping coefficients of the bearing bracket, in *X*-direction and *Y*-direction, are respectively given by k_{bx} and k_{by} and c_{bx} and c_{by}.

Mechanical seal were considered isotropic ($k_{xx} = k_{yy} = k$ and $c_{xx} = c_{yy} = c$), with negligible cross-coupling effects ($k_{xy} = k_{yx} = 0$ and $c_{xy} = c_{yx} = 0$), The shaft relative vibrations measured by proximity transducers are given by $u_x=(x_s– x_b)$ and $u_y=(y_s- y_b)$, while the bearing absolute vibrations measured by piezoelectric accelerometers are $\ddot{x}_b$ and $\ddot{y}_b$.

When the shaft, due to the eccentricity caused by the external and forced preload of the misalignment, constricts and approaches the seal wall off-centre, the rigidity of the oil film increases, as can be seen in the Figure 10 and its "spring systems" rotates at angular speed λΩ,[10].

Generally, in the case of seal lubricated by fluid film, adopts the strategy that the rotating machine represents a system, that include elastic elements as well as the fluid such as in bearings, seal, or rotor to stator peripheries, including pump/compressor, impeller/diffuser and clearances[11]. The fluid forces model is based on the rotor/relation/relative forward circumferential flow strength, so the average angular velocity of the flow is a fraction of the rotor rotative speed (λ) that is a decreasing function of the rotor eccentricity.

In summary, the physical phenomena in rotor to stationary part radial filled with the fluid are very similar, the fluid gets involved in the circumferential motion that creates tangential destabilizing forces, and the final results are measurable mostly vibrations subsíncronas of the rotor.

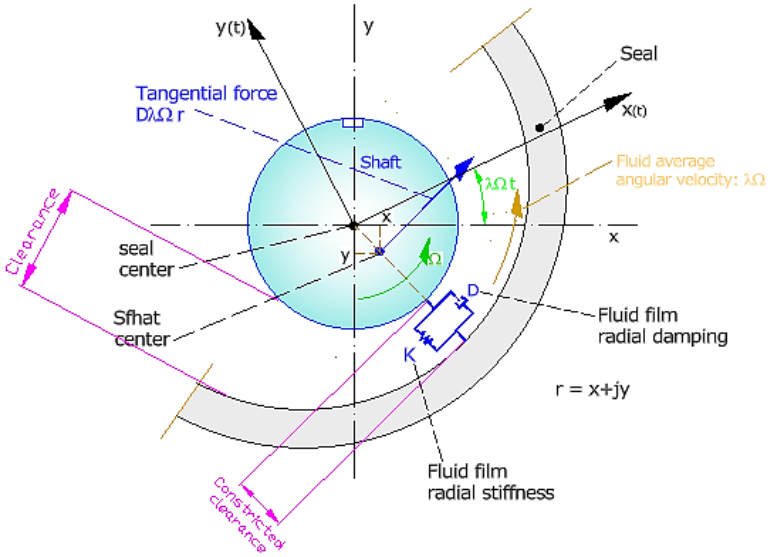

Figure 10: Fluid film model. Limited radial clearance.

2.1Misalignment Centerline

A very significant effect of misalignment is the aforementioned change in the position of the center of the shaft within its bearing or seal, at each end of this shaft, since the bearing is the element most pronounced in restriction of radial forces. The radial misalignment preload, therefore, will change this position of the center of the shaft and its direction will always be one that allows the shaft to undo that misalignment as much as possible. We will have the graphs of the Figure 11.

The plot a) of Figure 11 corresponding to bearing 3a, where the rotor is started and it is observed how it goes from a low position in the bearing to rise towards the center of that bearing. In the case of bearing 3b and mechanical seal, subjected to a misalignment preload, by means of springs "5" of the Figure 5, the shaft is vertically constricted to the lowest positions of the hole of that bearing and the same happens in the mechanical seal, lubricated by a pressurized oil film.

This explains the throttling of the orbit in bearing 3b and in the mechanical seal, the preload forces the shaft against the seal and bearing support, thus increasing dynamic stiffness. In the case of bearing 3a, it is also explained that the orbit is more circular, as the rotor shaft ends up being positioned near the center of the hole and the dynamic stiffness will decrease.

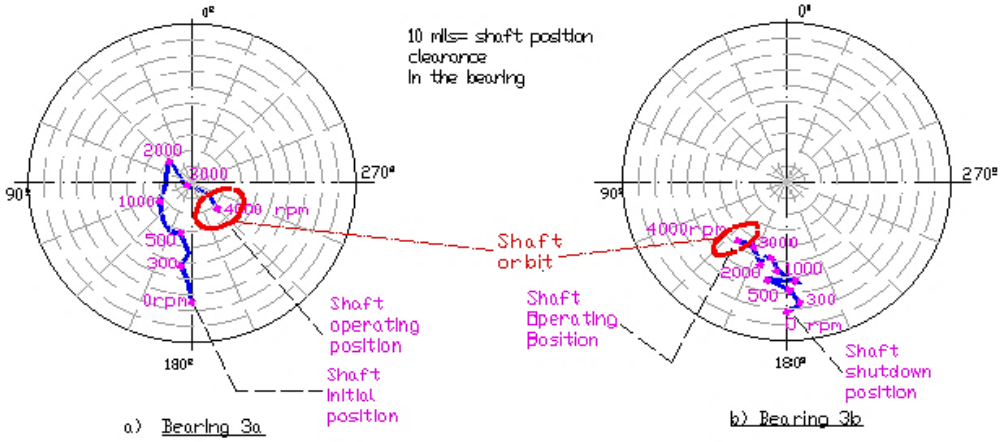

Figure 11: a) Bearing 3a, startup shaft centerline plot. b) Bearing 3b, shaft centerline.

The signal obtained from the induction and seismic transducer, while it is located in position 11 of the Figure 5, and before subjecting the rotor to misalignment preload, when the rotor start is that of the Bodé diagram of the

Figure 12, in which it is observed how the signal of the seismic transducer on the pedestal is lower than that obtained with the proximity transducer, among other reasons, because bearings 3a and 3b of the Figure 5 are somewhat flexible antifriction bronze bearing, and do not transmit to the pedestal all the vibration that the rotor has relative to the support. The amplitude reveals that there is a resonance at 2260 rpm.

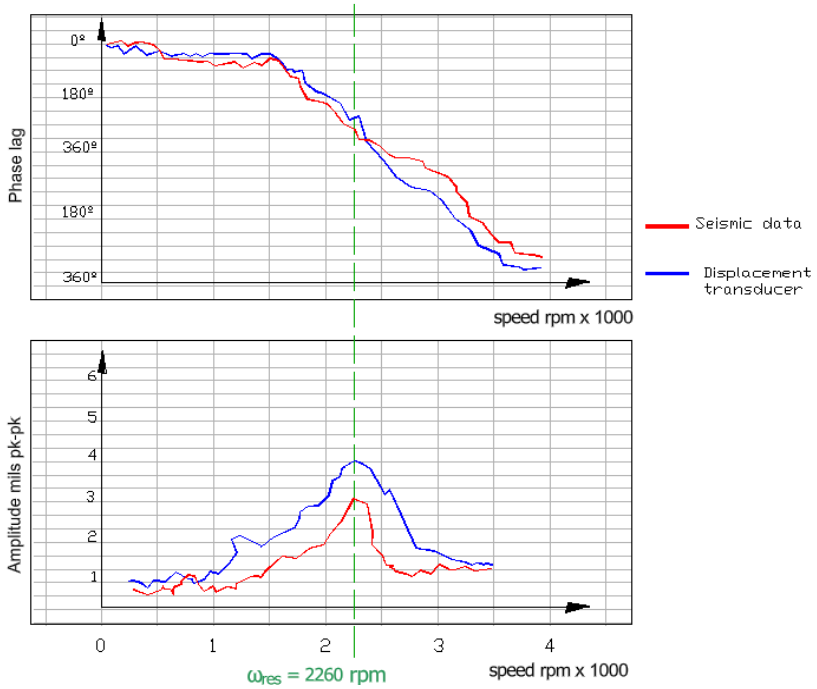

Figure 12: Bearing 3a. Bode. Seismic transducer at location 11. 1X response

2.2Misalignment Dynamic Stiffness

Once the misalignment load has been entered, the Bodé diagram obtained is that of Figure 13 to 1X response, from mechanical seal, in which it is observed that due to the increase in rigidity, the resonance value increases from 2260 rpm to 2450 rpm, $\Omega_{res}=\sqrt{(K/M)}$. It is also indicated in this figure, as depending on the increase in rigidity of the vertical misaligned plane y-y, the greater the ratio of that increase k_{yy}/k_{xx}, with respect to the horizontal plane, the greater the amplitude of vibration generated in the resonance frequency. With the seismic transducer on the pedestal, obviously none of these signal differences are picked up.

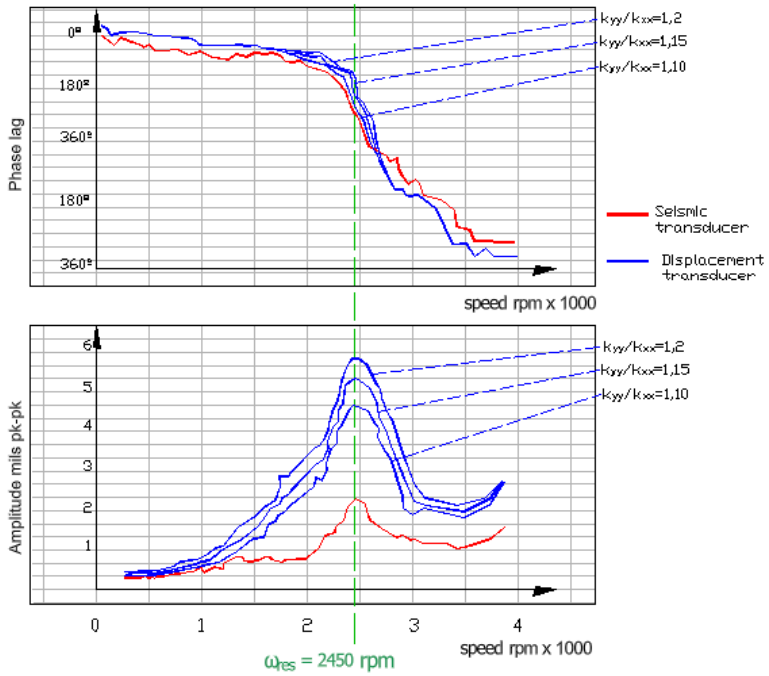

Figure 13: Mechanical seal. Bode. Seismic transducer at location 13. Misalignment preload

These misalignment situations frequently occur when cold assembly and alignment are performed. Seismic transducers announce the problem of increased vibration, but they do not provide information on the change in rotor characteristics or the causes that can cause this increase in vibration, as proximity transducers do with the modification of the eccentricity of the center of the shaft or with the modification of dynamic stiffness different in the two directions.

The induction transducers make it possible to obtain the dynamic stiffness in each support that can be calculated according to as described in [12]. Also confirms the increase in dynamic stiffness and consequently in resonance: $\omega_{res} = \sqrt{K/M}$, as shows in the Figure 14, where $K_D$is a parabola for the component of the real dynamic stiffness K_D = K-MΩ^2. In this figure it is observed how this K_D component, that is determined by extending the parabola to the ordinate axis (Ω = 0 rpm), is 13,80 KN/m, greater than the original date of 10,65 KN/m, Figure 15, while in bearing 3a, as the shaft goes to the center of the clearance, the dynamic stiffness will decrease a little.

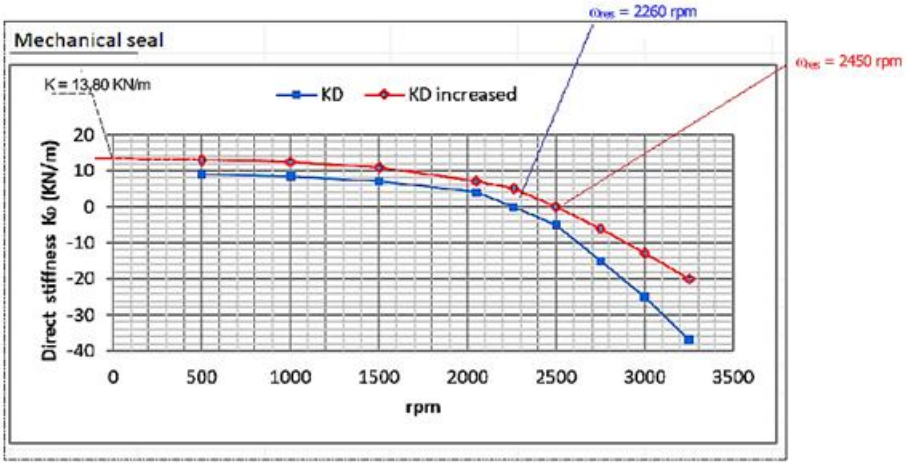

Figure 14: Mechanical seal. Dynamic stiffness

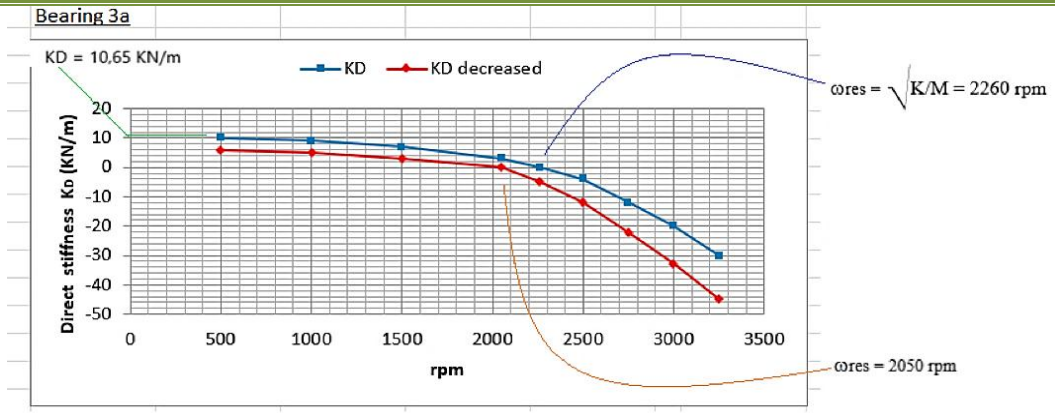

Figure 15: Bearing 3a. Dynamic stiffness.

2.3Misalignment 2x Response

On the other hand, misalignment is known to produce a significant 2X response, almost as large as 1X. The 2X answer must appear because the shaft, being a cylinder within another that is the bearing or seal, when it hits one side of the bearing, makes two trips upwards (once for each hill) in a single complete turn (Figure 16).

The motion of a shaft with this phenomenon, for an exclusive misalignment in the vertical plane, was represented bythe equations (3) and (4) and its solutions by (5) and (6), [2]. This is not the case in the non-misaligned x-plane, where the amplitude and phase angle are:

$$A_x = \frac{m\, r\, \Omega^2}{\sqrt{(K - M\Omega^2)^2 + (D\Omega)^2}}$$
$$\alpha_x = \delta + \text{arc tg}\left(\frac{D\Omega}{M\Omega^2 - K}\right) \quad (11)$$

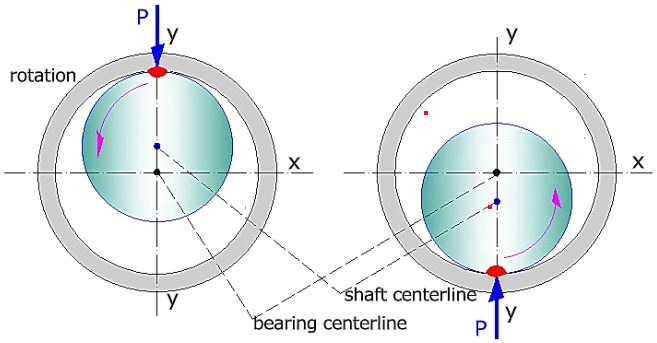

Figure 16: Double impact of the shaft on the bracket.

The phase angle to 1X response is:[2]

$$\alpha_1 = \delta + \text{arc tg}\left(\frac{D\Omega + K_n\, A_2 \sin\varepsilon}{M\Omega^2 - K - 2K_n A_0 - K_n A_2\, \cos\varepsilon}\right) \quad (12)$$

Where:

$$\varepsilon = \text{arc tg}\left(\frac{2D\Omega}{4M\Omega^2 - K - 2K_n A_0}\right) \quad (13)$$

$$\alpha_2 = 2\,\alpha_1 + \varepsilon - 90° \quad (14)$$

When the rotation speed is very low, close to zero, ε⟶ = and $\alpha_1 = \delta$, so at that low speed, the phase angle of the 2X response will be: -90º + δ, and the Bodé diagram that is obtained is that of the Figure 17.

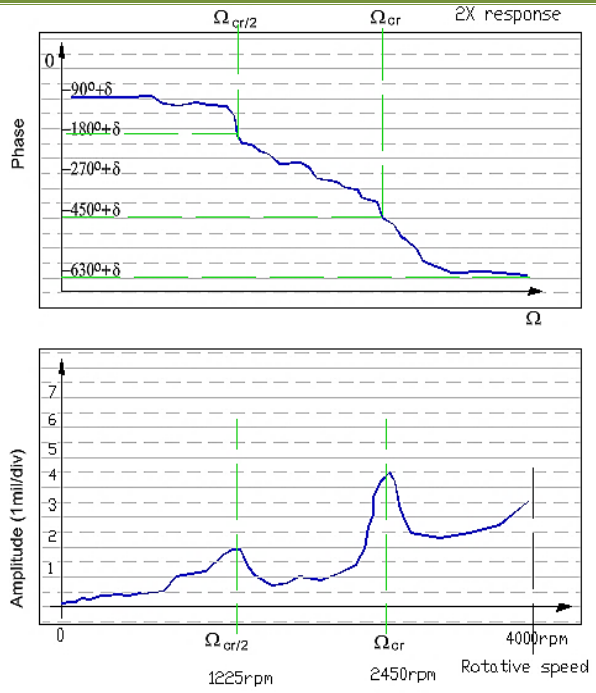

Figure 17: 2X response.

This Figure 17 obtained in the test rotor, once the forced preload of misalignment has been introduced, in the proximity transducers "12" to the mechanical seal of the Figure 5, thus confirming the phenomenon of this misalignment. It can be seen in this figure how in the 2X response two resonance amplitudes appear at $\Omega_{crt}/2$ and Ω_{crt}, in addition to the two corresponding phase changes.

The mathematical model described in equations (3) to (6)[2], is very simple and does not take into account possible signal couplings in other directions but clearly identifies the symptoms of the 2X response as a function of other parameters and, above all, of the rotational speed.

Another presentation that clearly shows the presence of the 2X response is the cascade spectrum during the startup from the rotor[13]. This transit data format displays the spectral behaviour of the rotor vibration over a range of operating speeds. The plot´s vertical axes are two, one is the rotor speed and other is vibration amplitude, while the horizontal axis is the vibration frequency. Diagonal lines are drawn to show multiples and submultiples of the running speed, 0.5X, 1X, 2X, 3, etc. the running speed, according to Figure 18 and Figure 19.

The Figure 18shows the typical characteristics of a misaligned plane, exclusively, and that in this case is the vertical plane taken data from the 12V transducer of the Figure 5, and which are:

- Simultaneity of 1X and 2X response.
- General increase of the 1X response with the speed, in the 12V transducer respect to the 12H, because in the vertical plane, with the application of the radial load imposed, a displacement of the centre of the shaft appears that causes an imbalance of mass greater than which may to produce only the anisotropy in the cross section of the shaft (Figure 18).
- The misalignment show up exclusively in the vertical direction, as an external force that does not manifest itself in the horizontal direction any more than it will correspond to the coupling of both 12V and 12H signals, so in the 12H transducer the amplitude of the 2X response is only just modified, as can be seen in the Figure 19.
- In the 12V transducer a peak of vibration amplitude is shown at the rotation speed equal to 1100 rpm, coinciding with the value of half of the first natural frequency in the 1X response of the vertical plane of misalignment, because the imbalance of mass produced by this displacement of the centre of the misaligned shaft already manifests itself at low speeds (Figure 18).
- Always, in the case of misalignment, we will also have an important axial vibration of the order of half the value of the radial amplitude.

The Figure 19 shows the data collected from the 12H transducer, in the non-misaligned horizontal plane, in which only an important signal of the 1X response is observed in the resonant frequency and some other signal in other multiples, due to the coupling between planes.

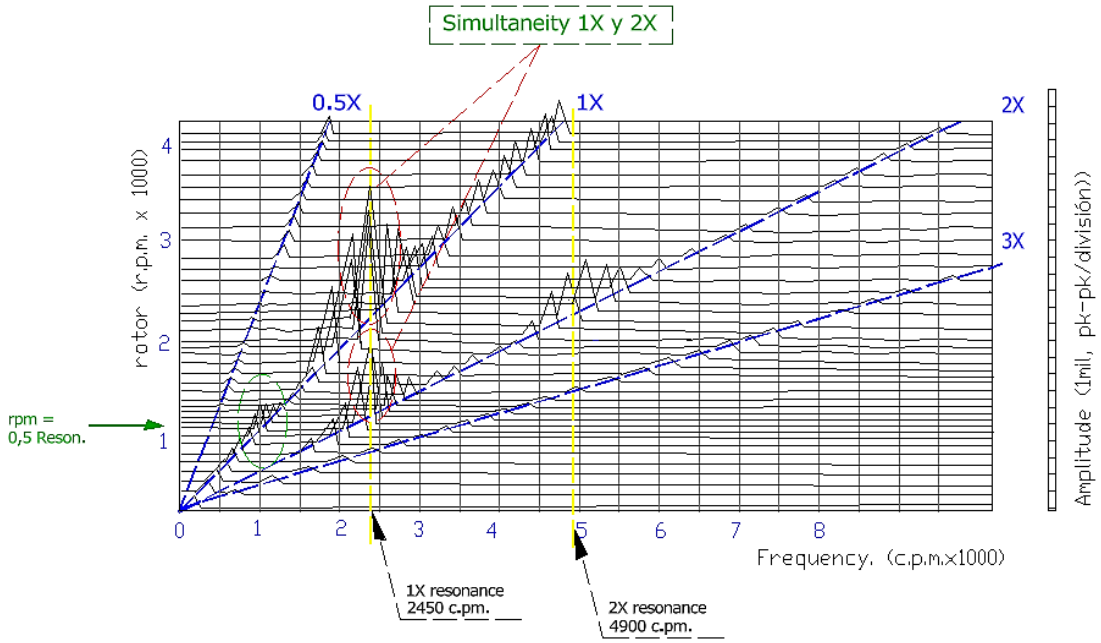

Figure 18: 12V Transducer. Cascade spectrum.

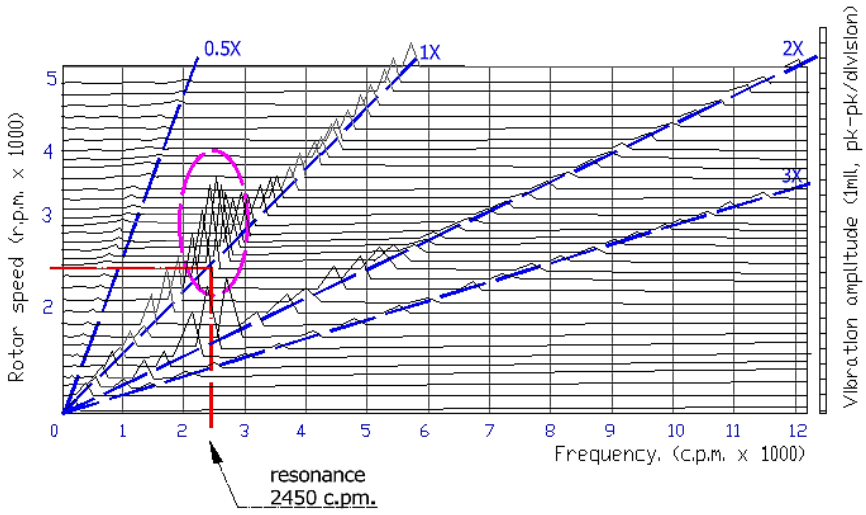

Figure 19: 12V Transducer. Cascade spectrum.

3. Conclusions

It should be understood that an acting radial load on a rotor operating at constant speed causes synchronous response, with possible harmonic components, which produce cyclic forces that origin tensions in the fibres of the shaft and/or rotor, whose number of cycles can reach the fatigue limit and can develop in a rupture of this rotor or shaft.

The design of vibration monitoring must have two criteria: one, that an alarm is given to protect the machine and another, that it provides sufficient information to know the causes of the increase in vibration. It is shown in this study that the installation of only the seismic transducer provides alarm for high vibration but requires the installation of induction transducers placed at 90º, if the causes of this vibration are to be known, as results from this study.

The best way to implement this is during the design and manufacture of the machines. The information of the parameters of the machines, such as the start-up and stop data of the machines, Bode, Nyquist, cascade

spectrum, natural frequencies, vibration mode, position of the center of the shaft must be shared with the operators of the facility.

Designers must know the rules of online monitoring and include in the design and manufacture of machines the appropriate locations of the necessary transducers.

Refernces

[1]. A. Muszynska, "Mathematical model of misaligned rotor," in Taylor & Francis, *Rotordynamics.* ISBN 0-8247-2399-6, New York, 2021, pp. 185-186.

[2]. A. Muszynska, "Misaligment Model," *Bently Rotor Dynamic Research Corporation. BRDRC Report No. 1,* Minden, Nevada. USA, 1999.

[3]. R. S. M. K. S. Kumar, "A State-of-the-Art Review on the Misalignment, Failure Modes and Its Detection Methods for Bearings. https://doi.org/10.1007/s12647-022-00605-x," *MAPAN. Journal of Metrology Society of India., vol. 38,* pp. 265-274, 2023.

[4]. P. G. L. Dal Bo, "Energy harvesting with electromagnetic and piezoelectric seismic transducers: Unified theory and experimental validation," *Journal of Sound and Vibration, vol. 433, no*. https://doi.org/10.1016/j.jsv.2018.06.034, pp. 385-424, 2018.

[5]. *Bently Nevada. Rotor Kit.,* 2016.

[6]. C. Hatch, R. Jesse and J. Whiteley, "Machinery Diagnostics Dynamic Stiffness in whirl and whip," *Bently Nevada Technical Training Departament,* Skelmersdale, UK, 2016.

[7]. A. Muszynska, "2.4.1.4 Displacement Transducer," in Taylor & Francis Group, *Rotordynamics,* Boca Raton, 2005, pp. 79-85.

[8]. P. Schaldenbrand, "https://community.sw.siemens.com/s/article/Orbit-Plots," *Siemens Digital IndustriesSoftware,* 27 Feb 2021. [Online]. [Accessed 18 November 2024].

[9]. R. D. M. a. A. C. N. Geraldo Carvalho Brito Jr., "Experimental Estimation of Journal Bearing Stiffness for Damage Detection in Large Hydrogenerators," *Shock and Vibration, vol. 1, no. Article ID 4647868,* p. 17, 2017.

[10]. D. Childs, in Jhon Wiley&Sons Inc., "*Turbomachinery Rotordynamics,*", New York, 1993.

[11]. A. Muszynska, "Model testing of rotors with fluid interaction," *International Journal of rotating machinery, vol. 1, no. 2,* 1995.

[12]. B. Fraga De Cal, "Study of the stability margin and its connection with the dynamic stiffness applied to a tidal turbine," *International Journal of Latest Engineering Research and Applications (IJLERA), vol. 04, no.01,* pp. 01-11, 2019.

[13]. P. Goldman, "Application of full spectrum to rotating machinery diagnostics," *Orbit. Bently Nevada Corporation, vol. 20, no. 1,* pp. 17-21, 1999.

